

# PCCP

Accepted Manuscript



This is an *Accepted Manuscript*, which has been through the Royal Society of Chemistry peer review process and has been accepted for publication.

*Accepted Manuscripts* are published online shortly after acceptance, before technical editing, formatting and proof reading. Using this free service, authors can make their results available to the community, in citable form, before we publish the edited article. We will replace this *Accepted Manuscript* with the edited and formatted *Advance Article* as soon as it is available.

You can find more information about *Accepted Manuscripts* in the [Information for Authors](#).

Please note that technical editing may introduce minor changes to the text and/or graphics, which may alter content. The journal's standard [Terms & Conditions](#) and the [Ethical guidelines](#) still apply. In no event shall the Royal Society of Chemistry be held responsible for any errors or omissions in this *Accepted Manuscript* or any consequences arising from the use of any information it contains.

# Site-dependence of van der Waals interaction explains exciton spectra of double-walled tubular J-aggregates

Jörg Megow,<sup>1,\*</sup> Merle I. S. Röhr,<sup>2</sup> Marcel Schmidt am Busch,<sup>3</sup> Thomas Renger,<sup>3</sup>  
Roland Mitrić,<sup>2</sup> Stefan Kirstein,<sup>4</sup> Jürgen P. Rabe,<sup>4,5</sup> and Volkhard May<sup>4</sup>

<sup>1</sup>*Institut für Chemie, Universität Potsdam, Karl-Liebknecht-Straße 24-25, D-14476 Potsdam, F. R. Germany*

<sup>2</sup>*Institut für Physikalische und Theoretische Chemie, Universität Würzburg, Emil-Fischer-Straße 42, D-97074 Würzburg, F. R. Germany*

<sup>3</sup>*Institut für theoretische Physik, Johannes Kepler Universität Linz, Altenberger Straße 69, AT-4040 Linz, Austria*

<sup>4</sup>*Institut für Physik, Humboldt-Universität zu Berlin,*

*Newtonstraße 15, D-12489 Berlin, F. R. Germany*

<sup>5</sup>*IRIS Adlershof, Humboldt-Universität zu Berlin,*

*Zum Großen Windkanal 6, D-12489 Berlin, F. R. Germany*

The simulation of the optical properties of supramolecular aggregates requires the development of methods, which are able to treat a large number of coupled chromophores interacting with the environment. Since it is currently not possible to treat large systems by quantum chemistry, the Frenkel exciton model is a valuable alternative. In this work we show how the Frenkel exciton model can be extended in order to explain the excitonic spectra of a specific double-walled tubular dye aggregate explicitly taking into account dispersive energy shifts of ground and excited states due to van der Waals interaction with all surrounding molecules. The experimentally observed splitting is well explained by the site-dependent energy shift of molecules placed at the inner or outer side of the double-walled tube, respectively. Therefore we can conclude, that inclusion of the site-dependent dispersive effect in the theoretical description of optical properties of nanoscaled dye aggregates is mandatory.

## I. INTRODUCTION

The investigation of electronic exciton energy transfer (EET) in huge supramolecular systems is of enormous interest for the understanding of processes taking place in both biological [1–3] and artificial [4, 5] light harvesting antennae systems and therefore topic of recent research. As an example chlorosomes from green sulfur bacteria which cover thousands of pigment molecules have been investigated only recently [6–8].

Various artificial light harvesting systems have been established and explored experimentally [9, 10] and were also investigated theoretically, such as giant molecular macrocycles [11, 12] or large complexes of tetrapyrrole type molecules [13, 14]. However, a appropriate theoretical treatment of such systems still remains challenging. In this work we focus on the proper description of the structural and optical properties of the tubular dye aggregate (TDA) of the amphiphilic cyanine dye named C8S3 [15], formed in aqueous solution, which have been discussed in several studies [4, 16–18].

Former cryogenic transmission electron microscope (cryo-TEM) images suggested that the dyes are arranged within a double layer structure similar to lipid membranes facing the hydrophilic groups, and hence the chromophoric units, towards the liquid medium inside and outside of the tube and hiding the hydrophobic alkyl chains from the aqueous environment [4, 16]. This building principle is illustrated in Figures 1 and 2.

In previous studies investigating the double-walled tubular J-aggregates the linear optical spectra were explained theoretically by a parameterized Frenkel exciton Hamiltonian [19–21]. Therefore, the tubes were modelled by two telescoped tubes of dye molecules. For each cylinder independently a regular and distortion free lattice of dyes was assumed with two molecules per unit cell where every dye was represented by an extended dipole [5, 18, 22]. All energy shifts in the spectra were attributed to excitonic coupling while solvent shifts or dispersive energies were neglected or simulated by a constant shift. By the adjustment of mutual orientations, distances, and tilt angles, the absorption spectra were modelled in great detail. Also an assignment of bands that correspond to the inner and outer cylinder were provided. Notice, that in those works the structure of inner and outer cylinder was independent.

In contrast, highly sophisticated image reconstruction techniques revealed details of the structure of the tube wall indicating an organization of the dyes in ribbons that are helically winding within the wall [17]. The appearance of these ribbons requires a strong correlation between the arrangement of dyes within the inner and outer tube, which is not fulfilled by the model described above. On the other hand, the computation of optical spectra based on molecular dynamics (MD) simulations was approached in [23] for a single-walled tube and resulted in a too wide absorption line shape.

In this contribution we provide two new approaches to describe the corrected aggregate structure and spectra: first, the structure is modelled employing MD simulations. The start configuration is resolved to best approximate the appearance of highly resolved cryo-TEM images

\*Electronic address: megow@uni-potsdam.de

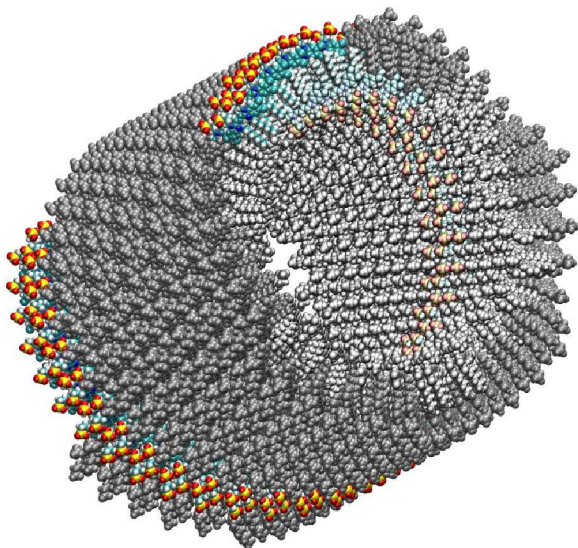


FIG. 1: Initial model of C8S3 TDA. One molecular ribbon of the outer cylinder is highlighted in color. The whole outer cylinder is drawn in grey and the inner one in light grey. (The figure was created using VMD [28].)

(cf. Fig. 1). A detailed model down to atomic resolution has been obtained that can be handled numerically and is stable over timescales of nanoseconds. Second, the linear absorption spectrum is calculated based on the MD structure taking into account transition densities for resonant excitonic interactions but also a full description of dispersive energies due to non-resonant interactions. The huge number of molecules within the slightly disordered aggregates account for disorder effects in the spectra. The results lead us to a new interpretation of the shift, and splitting into two fundamental bands of the absorption spectrum.

Considering bulk systems, the change of the molecular excitation energy due to an environmental influence is known as the gas-to-crystal shift. Electrostatic and inductive site energy shifts depend on the difference in charge density between the excited and the ground state of the molecule. If the latter is small, the leading contribution to the site energy shift is due to mutual polarization of different atoms (molecules): the van der Waals interaction or dispersive interaction. It was first proposed by London [24], to explain the attractive interaction between noble gas atoms (exhibiting closed electronic shells). Due to the Coulomb coupling between electrons in different atoms (molecules) a dynamic correlation in electronic motion stabilizes the coupled system and leads to reduction in energy. Since excited state wavefunctions are often more extended than the ground state ones, the dispersive shifts of excited state energies are usually larger than those of electronic ground states leading to a redshift of the transition energy [36]. It is important to note that the dispersive shift also includes the interaction with all other molecules of the environment.

Usually, dispersion effects of the surrounding medium are taken into account by assuming a single value for the molecular excitation (site) energy in order to place the whole absorption spectrum in the correct wavelength region. This implies the use of a constant transition energy shift. In the case of a nano-structured system the polarizability of the environment may strongly depend on the molecular position. Accordingly, the excitation energy shift does not remain a constant but becomes site-dependent. If this shift overcomes the strength of the resonant EET (excitonic) coupling it affects significantly the spectrum of excitation energies. We note, that such site-dependent dispersive energy shifts have been calculated for aggregates of Rydberg atoms in [25]. Here we utilize a method that is applicable to molecular aggregates.

It will be shown in the following that the separation of the two low-energy absorption bands as reported in [5] is mostly due to different dispersive shifts of the molecular excitation energy in the inner and the outer wall of the TDA. On the other hand, the resonant excitonic coupling is found to have less impact on the separation of these two bands.

## II. RESULTS

To achieve a consistent explanation of the TDA absorption spectrum, our subsequent considerations will be based on a spatial structure that is obtained by MD simulations starting from a configuration resembling highly resolved cryo-TEM images [17]. The simulated system included 828 C8S3 molecules, 74116 water molecules and 9242 methanol molecules in a box of  $17 \times 17 \times 12.6$  nm with periodic boundary conditions [26]. The simulations are extended up to 7 ns. Here, it is essential to ensure that the solvent density inside the tube coincides with that outside. After an equilibration time of a few 100 ps the TDA structural parameters were found to stay constant, indicating a stable structure of the aggregate. In Fig. 2 the structure after 7 ns of simulation is shown.

In the case of a TDA of C8S3, due to the curvature the environment in proximity of the dye molecules has a different composition in terms of number of dye molecules per volume. This mainly depends on the molecule either being located in the outer wall or in the inner wall. This effect is indicated in the lower panel of Fig. 2 by the circles showing the close environment for two dyes within the top view of a MD simulated aggregate. This circles with a radius of about 2 nm around the center of the molecular transition dipole moments indicate the close environment of the dyes which contributes most (>99%) to the dispersive energy shift.

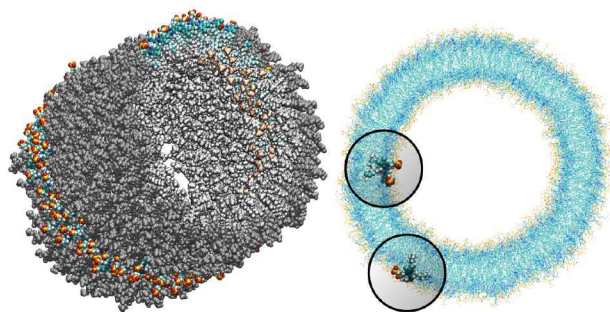


FIG. 2: MD aggregate after 7 ns of simulation. Upper panel: side view according to Fig. 1. Lower panel: Top view of the C8S3 TDA with a dye molecule in the inner cylinder and the outer cylinder highlighted. The spheres around the highlighted molecules have a radius of 2 nm. They indicate a volume that includes all dye molecules that contribute more than 99% of the contributions to the dispersive energy shift. Note that more dye molecules are within this sphere for the molecules at the inner wall than those for the outer wall. (The figures were created using VMD [28].)

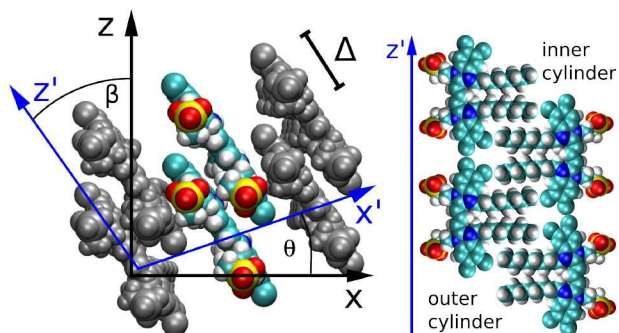


FIG. 3: Internal structure of the C8S3 TDA. Left panel: molecular ribbon with two molecules forming a unit cell. The internal coordinate system is drawn in blue. Right panel (schematic): orientation of the C8S3 dyes in the outer (left) and inner (right) cylinder. (The figures were created using VMD [28].)

### A. TDA structure

According to the cryo-TEM data, the whole TDA structure consists of six ribbons, turned around a common axis, forming an inner and an outer cylinder (see Fig. 1). Both cylinders have the same periodicity (twists per aggregate length), which is 12.7 nm. The width of a single ribbon amounts to 20.1 Å for the outer cylinder and 19.5 Å for the inner cylinder (they differ due to the different screw angles). The extension of a single C8S3 molecule along the transition dipole axis is 20.8 Å. We assumed an orientation of the molecules with dipole moments parallel to the cylinder surface what is confirmed by our MD simulations. These ribbons then wind up with a screw angle  $\theta$  and the molecules have to be tilted against the  $z$ -axis of the tube by an angle  $\beta$  (see Fig. 3).  $\theta$  amounts to 18.3° for the outer and 23.0° for the inner cylinder.  $\beta$  amounts to 34.5° for the outer and 44.3° for

the inner cylinder. We note that no exact value for  $\beta$  can be extracted from the cryo-TEM images.

The mean distance of neighboring molecules is 5 Å within both cylinders, measured as the distance between the molecular centers of the  $\pi$ -electron system. The closest distance between two molecules is about 4 Å. The distance between neighbored molecules varies due to the angle between them. We also tried simulations with closer packed molecules. They were not stable since some of the atoms came too close to each other. The distance between the two cylinders amounts to 13 Å (measured with respect to the centers of the molecular  $\pi$ -electron systems).

Our model assumes two molecules per unit cell. Therefore, a mutual displacement  $\Delta$  as indicated in Fig. 3 was introduced by hand with a value of  $\Delta = 9$  Å.  $\Delta$  was chosen in order to obtain the correct absorption spectrum (see below) and is the only free parameter in our model. Due to the displacement  $\Delta$  our model includes two molecules per unit cell. The structural stability of the TDA for such a mutual molecular displacement has been confirmed by extended MD simulations. We note, that using  $\Delta = 0$ , a structure model consistent with [17] results in an H-aggregate-like absorption spectrum.

For comparison, a MD simulation, basing on the structure model presented in [5] was employed. It is specific for that model, that the molecular structures of the inner and outer wall differ and furthermore are completely independent from each other, *i.e.* there is no correlation between the respective molecular positions. Additionally, the molecules are arranged in a Herringbone-like structure, also resulting in 2 molecules per unit cell. However, by performing MD simulations, this model turned out to be unstable, since the tubes disintegrated with time. Therefore, we conclude that the strong correlation between inner and outer tube as it is provided by the model of the two-layer ribbons reduces the system's free energy and stabilizes the structure significantly.

### B. Frenkel exciton Hamiltonian

Having determined the TDA structure we can turn to a computation of the resulting excited electronic states. Singly excited states of the TDA as detected in linear absorption measurements can be deduced from the standard Frenkel-exciton Hamiltonian

$$H_{\text{exc}} = \sum_m \mathcal{E}_m |\phi_m\rangle \langle \phi_m| + \sum_{m \neq n} \mathcal{J}_{mn} |\phi_m\rangle \langle \phi_n|. \quad (1)$$

In its diagonal part it covers the so-called site energies  $\mathcal{E}_m$  (excitation energy of molecule  $m$ ). The off-diagonal part is formed by the excitonic coupling  $\mathcal{J}_{mn}$  which resonantly transfers excitation energy from one dye molecule to the other. The  $\phi_m$  are molecular product states with molecule  $m$  in the first excited state  $\varphi_{me}$  and all other molecules in the ground state  $\varphi_{ng}$ . The restriction to a single excited state becomes possible since higher excited

states are energetically sufficiently far away. The overall ground state  $\phi_0$  is a product of all  $\varphi_{ng}$ . A ground state part  $E_0|\phi_0\rangle\langle\phi_0|$  does not appear in the Hamiltonian since we set  $E_0 = \sum_m E_{mg} = 0$ .

The excitonic coupling  $\mathcal{J}_{mn}$  coincides with  $J_{mn}(eg, eg)$  which is a particular example of the general two-molecule Coulomb matrix element  $J_{mn}(ab, b'a')$ . The electronic quantum numbers  $a$  and  $a'$  belong to molecule  $m$  and  $b$  and  $b'$  to molecule  $n$ . The matrix element appears as the Coulomb interaction of the charge density  $n_{aa'}^{(m)}(\mathbf{x})$  of molecule  $m$  and the charge density  $n_{bb'}^{(n)}(\mathbf{y})$  of molecule  $n$ . If, for example,  $a \neq a'$  the density  $n_{aa'}^{(m)}(\mathbf{x})$  is exclusively determined by the electronic transition density  $\rho_{aa'}^{(m)}(\mathbf{x})$  [31]. For concrete computations the continuous charge densities are replaced by discrete atomic centered partial charges and partial transition charges [37]. The unscreened excitonic coupling is between +30 and +40 meV for neighbored molecules within the same ribbon. It is between -40 and -30 meV for neighbored molecules of two adjoined ribbons. Since each molecule couples strongly to three molecules of each adjacent ribbon (cf. Fig. 3) the J-aggregate character dominates.

### C. Curvature induced dispersion shifts

The minimal version of the exciton Hamiltonian introduced so far has to be improved by a consideration of further couplings among the molecules which may change the site energies as well as the matrix elements of the excitonic coupling [27]. Electrostatic couplings due to permanent charge distributions in the ground and the excited state of the dye molecules result in the shift  $\Delta\mathcal{E}_m^{(el)} = \sum_k [J_{mk}(eg, ge) - J_{mk}(gg, gg)]$  of site-energy  $\mathcal{E}_m$  (contributions due to solvent molecules are incorporated in the  $k$ -sum [29]).

The charge densities of the ground and excited states polarize the environmental molecules, a polarization that reacts back on the considered molecules and introduces the site energy shift  $\Delta E_m^{(pol)}$ . A third type of site energy shift arises from the mutual Coulomb coupling of transition densities and is termed dispersive site energy shift  $\Delta E_m^{(disp)}$  [31, 32]. Introducing the dispersive change of the molecular energy referring to state  $\varphi_{ma}$  as  $\Delta E_m^{(disp)}$  we obtain (remember  $a = g, e$ ) [27]

$$\Delta E_{ma}^{(disp)} = - \sum_k \sum_{f, f'} \frac{|J_{mk}(f'f, ag)|^2}{E_{mfa} + E_{kf'g}}. \quad (2)$$

The  $f$  and  $f'$  count all higher excited energy levels ( $f, f' > e$ ), the  $E_{mfa}$  and  $E_{kf'g}$  are the transition energies of molecule  $m$  and  $k$ , respectively, and  $J_{km}(f'f, ag)$  denotes the respective Coulomb matrix element. Such matrix elements relate transitions in the considered molecule  $m$  to transitions in all other molecules labeled by  $k$ . According to the actual position of molecule

$m$  in the TDA the  $k$ -summation notices the concrete conformation of dye molecules around molecule  $m$ . Consequently, the overall site energy shift follows as  $\Delta\mathcal{E}_m^{(disp)} = \Delta E_{me}^{(disp)} - \Delta E_{mg}^{(disp)}$ .

Hence, the site energies  $\mathcal{E}_m$  are shifted in total by

$$\Delta\mathcal{E}_m = \Delta\mathcal{E}_m^{(el)} + \Delta\mathcal{E}_m^{(pol)} + \Delta\mathcal{E}_m^{(disp)}. \quad (3)$$

We note that Eq. 3 includes all energetic (static) disorder explicitly. For the present C683 chromophore we find that  $\Delta\mathcal{E}_m^{(disp)} \gg \Delta\mathcal{E}_m^{(el)}$ . While  $|\Delta\mathcal{E}_m^{(el)}|$  is in the order of 10 meV,  $|\Delta\mathcal{E}_m^{(disp)}|$  is in the order of over 500 meV. This result is understood by noting the comparably similar charge densities of the ground and excited electronic state (differential dipole moment is about 1 D [30]). Since we expect  $\Delta\mathcal{E}_m^{(el)}$  in the same order of magnitude as  $\Delta\mathcal{E}_m^{(pol)}$ , we get  $\Delta\mathcal{E}_m^{(disp)} \gg \Delta\mathcal{E}_m^{(pol)}$ . Therefore, we neglect  $\Delta\mathcal{E}_m^{(pol)}$  in our calculations.

In order to determine the energy shifts of every individual molecule within the aggregate the expression, Eq. (2), has to be transformed into a tractable form to compute its dependence on the mutual position of the coupled molecules. Here, we follow Ref. [27]. Accordingly, in a first step  $J_{mk}(ag, f'f)$  is replaced by an expression of two interacting extended dipoles with charges  $\pm q(fa)$  and  $\pm q(f'g)$ . Electronic structure computations indicate that these dipoles are oriented along the elongated part of the cyanine dye. Assuming uniform extension of all extended dipoles we may write  $\Delta\mathcal{E}_m^{(disp)} = -Q \sum_k V_{mk}^2$  where  $V_{mk}$  represents all geometrical factors, *i.e.* the Coulomb interaction of both extended dipoles but with unit charges. Concrete values of the latter are included in the factor  $Q = \sum_{f, f'} q^2(fe)q^2(f'g)[1/(E_{fe} + E_{f'g}) - 1/(E_{fg} + E_{f'g})]$ , where  $E_{fe}$  ( $E_{f'e}$ ) and  $E_{fg}$  ( $E_{f'g}$ ) are the transition energies between the first excited and the ground states of the isolated monomers, respectively, and the higher excited states.

By further proceeding in line with Ref. [27] we do not determine the  $Q$ -factor by a direct computation, which would be not accurate enough, but by using experimental data on transition energy shifts in non-polar solvents. If the solvent is described by a dielectric continuum with refractive index  $n$ , the shift can be approximately obtained as [33, 36],

$$\Delta\mathcal{E}_m^{(disp)} = -\mathcal{F} \frac{n^2 - 1}{2n^2 + 1}, \quad (4)$$

which describes the shift induced by a polarizable environment. If a value for  $\mathcal{F}$  is available and if we know  $n$  for a random arrangement of C8S3 molecules we can determine the site-energy shift. Noting previously published spectra of a similar compound [34] we may deduce  $\mathcal{F} \approx 1.43$  eV, and a gas-phase transition energy follows as  $E_{gp} = 2.64$  eV. Moreover we take  $n_{TDA} \approx 1.78$  [35]. According to [27, 36] we have to chose the long wave-length limit of the refractive index resulting in  $\Delta\mathcal{E}_m^{(disp)} \approx -0.43$

eV. Identifying this value with  $-Q \sum_k V_{mk}^2$  we may deduce  $Q$  after carrying out the  $k$ -summation. Since the experimental value of  $\Delta\mathcal{E}_m^{(\text{disp})}$  corresponds to a random arrangement of the molecules (they have to form a structureless polarizable continuum) we determine  $Q = 7.61 \text{ eV\AA}^2$  by introducing an averaged expression  $\langle \sum_k V_{mk}^2 \rangle$ . It assumes random mutual orientation of the molecules but at a mean density typical for the TDA.

This value of  $Q$  is further used to calculate the dispersive site-energy shifts of all molecules within the TDA. The used approximation leads to a significant fluctuation of the individual energy shifts. This is mainly caused by the extended dipole approximation, which is a good approximation on average. However, individual couplings may vary by up to 30 %. Therefore, we average the shifts for the inner and the outer cylinder separately. That way, the artificial fluctuation due to the utilization of the extended dipole approximation disappears.

The solvent effect on the dispersive site-energy shift  $\Delta\mathcal{E}_m^{(\text{disp})}$  (Eq. 4) was neglected because of the small refractive index of the solvent ( $n \approx 1.33$ ) and the comparably restricted contact area between the solvent and the dye molecules. For comparison: a dissolved monomer is shifted by about 0.3 eV (cf. Eq. 4). The C8S3 molecules within the tube however, obtain a smaller dispersive shift, since they are mostly surrounded by other C8S3 molecules (cf. Fig. 2). Assuming that a molecule within a wall interacts with less than half of the solvent molecules than a monomer in solution one obtains an upper limit of below 0.15 eV for the solvent dispersive shift of C8S3 molecules within an aggregate. The dispersion shift due to solvent interaction is somewhat larger for molecules in the outer cylinder, since they have contact with more solvent molecules due to geometric reasons. Assuming that this solvent interaction shift will be about 10 – 15 % larger for molecules in the outer cylinder one obtains a reduction of the mutual energy splitting of the two J-aggregate bands by 0.02 eV (6 nm) at most.

Having discussed the change of the site energies due to dispersion of the environment we briefly comment on a related alternation of the excitonic coupling, *i.e.* we introduce screening to the non-diagonal elements of Eq. 1. Similar to the site-energy shift it results from an environmental dispersion (see *e.g.* [38]) which, in general, reduces the excitonic coupling  $\mathcal{J}_{mn}$  between two molecules to  $f_{mn}\mathcal{J}_{mn}$  [14, 38]. The prefactor  $f_{mn}$  can be approximated by a constant  $1/\epsilon = 1/n^2$  where  $n$  is the optical refractive index [14]. From the dispersive shifts of the inner and outer cylinder we calculated the respective refractive indices  $n_{\text{out}}$  and  $n_{\text{in}}$  for both cylinders. This was realized assuming the measured refractive index  $n = 1.78$  being an average value  $n = (N_{\text{out}}n_{\text{out}} + N_{\text{in}}n_{\text{in}})/(N_{\text{out}} + N_{\text{in}})$ ,  $N_{\text{out}} = 468$  and  $N_{\text{in}} = 360$  being the numbers of molecules in the outer and the inner cylinder, respectively. We obtain  $n = 1.89$  for the inner cylinder and  $n = 1.69$  for the outer cylinder. From the respective indices we yield screening factors for the coupling of two molecules within a certain cylinder.

We note that this site-dependent screening factors, used for reasons of consistency change our result only slightly, which can be explained by the rather small contribution of the excitonic couplings to the overall energy shifts.

For the coupling between two molecules located in different cylinders we take  $n = 1.78$ , getting  $f_{mn} = 0.35$  for the outer cylinder,  $f_{mn} = 0.28$  for the inner cylinder and  $f_{mn} = 0.32$  for molecules located in different cylinders, *i.e.* a noticeable reduction of the excitonic coupling. The somewhat larger screening factor for the outer cylinder results in a slightly decreased energy distance of the two J-aggregate peaks. The  $\mathcal{J}_{mn}$  were calculated via a coupling of transition partial charges (which have been somewhat rescaled to reproduce the measured transition dipole moment [37]).

#### D. Optical spectra

After determining the site-energies and excitonic couplings which define the exciton Hamiltonian  $H_{\text{ex}}$ , Eq. (1), in a proper way [39], a respective diagonalization results in exciton energies and wave functions. To account for a large spatial delocalization of the exciton wave function, the TDA which constitutes the Hamiltonian  $H_{\text{ex}}$  has been formed by five fragments of 12.7 nm length used in the MD simulations (further increasing of the number of fragments only induces a minor effect on the exciton spectrum). Since after 7 ns of MD simulations all molecular positions deviate from the ordered structure (see Fig. 1) structural disorder is accounted for. Moreover, the huge amount of molecules which contribute to  $H_{\text{ex}}$  and thus to the exciton spectrum introduce a self-averaging effect. Since it operates when computing the absorption line-shape (sum of the squared excitonic transition dipole moments times the energy conserving  $\delta$ -function) further disorder averaging is not necessary. Homogeneous broadening was introduced by replacing sharp transitions into the various exciton levels by individual Lorentz-curves with a linewidth of 3 nm (FWHM).

Respective results together with measured data are presented in Fig. 4. If dispersive effects are neglected only a single TDA band results, which is shifted slightly to longer wavelengths compared with the monomer absorption. The small red shift of about 10 meV (2 nm) is due to the screened excitonic coupling (it is about -10 meV between neighboring molecules belonging to adjacent ribbons). Calculating the absorption spectra separately for the outer and the inner TDA cylinder (yet neglecting dispersive effects) confirms almost vanishing splitting between the two exciton bands. Including, however, the site-dependent dispersion results in a line-shape that exhibits two separate bands and agrees quite well with the measured curves.

The calculated red shift of the exciton bands is too small by 0.1 eV (about 30 nm) compared to the experimentally measured shift (see Fig. 4). This 0.1 eV offset can be related to the ignored energy shift due to solvent

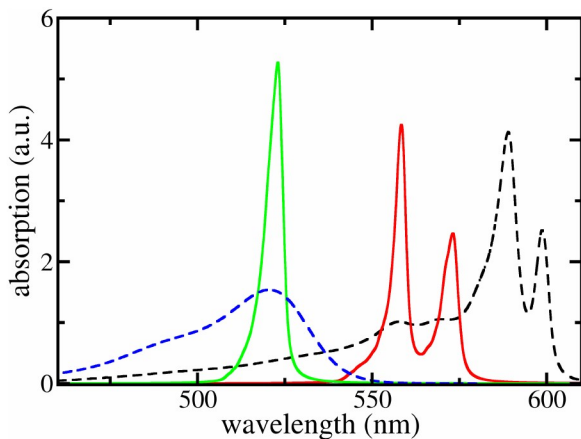


FIG. 4: Linear absorption spectra of a C8S3 TDA and of respective dye monomers. Black solid line: measured TDA absorption according to [5], blue dashed line: measured monomer absorption; green line: calculated TDA absorption neglecting the site-dependent dispersion; red solid line: completely calculated TDA absorption spectrum. No free parameters used, except for the slip  $\Delta$  in order to build the structure.

dispersion but also to the uncertainty when determining the linear factor  $\mathcal{F}$  and the gas-phase transition energy  $E_{gp}$ . This small unexplained shift has to be compared to the total energy shift of more than 0.5 eV relative to the  $E_{gp} = 2.64$  eV for which reason it can be accepted.

The treatment of solvent dispersion would also result in a slightly smaller energy difference between the two J-aggregate peaks (0.02 eV at most).

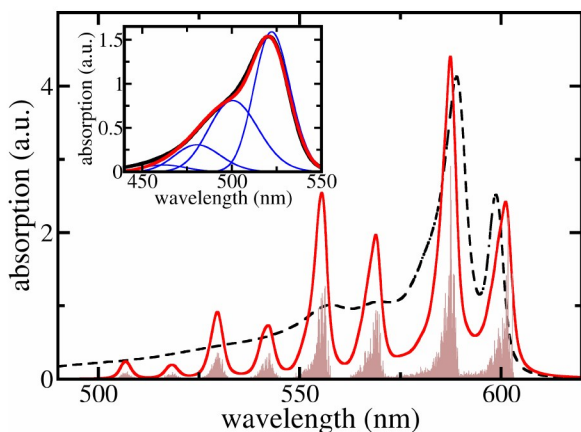


FIG. 5: Linear absorption spectra of a C8S3 TDA including a single representative intramolecular vibration per monomer (for details see text). Orange filled area: stick spectrum, red curve:  $\approx 3$  nm broadened stick spectrum, black dashed curve: measured absorption (cf. Fig. 4). The offset of 0.1 eV due to solvent dispersive shifts is included here. Inset: C8S3 monomer absorption. Red solid curve: computed absorption spectrum, black dashed curve: measured spectrum, blue solid curves: single vibrational level contributions.

Although the two long wavelength peaks of the TDA absorption are nicely reproduced in their spectral position and height, there is a considerable discrepancy around 550 nm. We briefly demonstrate that this discrepancy may be overcome by including C8S3 intramolecular vibrations. Fig. 5 shows respective results where a single representative and broadened vibrational mode per dye molecule has been used. Here, the 0.1 eV offset seen in Fig. 4 and supposedly caused by the neglect of solvent dispersive shifts is corrected. The coincidence of the computed monomer spectrum with the measured one as shown in the insert of Fig. 5 justifies the used vibrational energy of 0.1 eV, the Huang-Rhys factor of 0.74, and the line-broadening of  $\approx 35$  nm (it differs somewhat between the  $0 \rightarrow 0$  and  $0 \rightarrow \mu > 0$  transitions).

To calculate the whole TDA exciton spectrum by including a single vibrational mode per dye molecule we followed Ref. [41] and employed the so-called single particle approximation suggested therein (cf. also [27]). In this case, exciton states are introduced as  $\Phi_\alpha = \sum_{m,\mu} c_\alpha(m,\mu) \chi_{me\mu} \phi_m$ , where  $\chi_{me\mu}$  is the total vibrational wave function with  $\mu = 1\dots 3$  vibrational excitations in the excited state of molecule  $m$ . The expansion coefficients  $c_\alpha(m,\mu)$  are obtained via the diagonalization of the Hamiltonian, Eq. (1), which, however, has been extended on introducing vibrational contributions in the site energies and excitonic couplings. Now, vibrational satellites appear in the wave-length region around 550 nm which corresponds to absorption bands observed experimentally. The remaining differences between the calculated spectrum and the experimental data may be caused by the restriction to a single vibrational mode per C8S3 monomer. At this point we cannot exclude that other configurations are possible that lead to additional exciton bands and thus would reproduce more details of the spectra without involving vibrational modes. However, we can state that vibrational modes seem to strongly contribute to the spectra, what is due to the rather large Huang-Rhys factor. We can state further that our model is consistent regarding cryo-TEM figures, optical spectra, electronic structure calculations and MD simulations.

Finally, we would like to comment on a recent work where an environmentally induced heavy-tailed Lévi disorder is utilized to explain an additional low energy fluorescence band for drop-cast samples of 1-D J-aggregates [43]. Such a low energy band (90 meV below the general fluorescence band) could be attributed to a local conformation induced dispersion effect.

### III. CONCLUSIONS

A novel structure model for a C8S3 TDA together with site-dependent dispersive effects leads to a conclusive interpretation of the general features of the respective linear absorption spectra. Molecules in the

inner and outer cylinder of the TDA interact with a different environment, and accordingly their dispersive shifts differ. For the considered C8S3 TDA the excitonic coupling is particularly small due to screening and, thus, the observed absorption line splitting is mostly determined by environmental dispersive effects. This splitting, but not the overall shift of the spectrum, would vanish if the dyes formed an uncurved double-walled layer. Accordingly, we consider a long-wavelength absorption line splitting in TDAs a general feature, due to a curvature-induced site-dependent dispersive effect. While we ascribe the energy splitting of the main peaks mainly to an interaction of higher transition densities (non-resonant excitonic coupling), in previous work the

splitting was attributed to (resonant) excitonic coupling [5, 19–21]. It can be concluded that the site-dependence of dispersive energies is of key-importance to understand the optical properties of nanostructured molecular dye systems, such as nano-tubular light harvesting dye aggregates. We strongly suspect that this reasoning holds for nanoscaled molecular aggregates in general.

*Acknowledgments:* Financial support by the *Deutsche Forschungsgemeinschaft* through Sfb 951 and through project ME 4215/2-1 (J.M.) and by the *Austrian Science Fund* (FWF) through project P 24774-N27 (T.R.) are gratefully acknowledged.

- 
- [1] L. Zhang, D.-A. Silva, Z. Houdao, A. Yue, Y.J. Yan and X. Huang, *Nature Comm.*, 2014, **5**, 4170.
- [2] J. Strümpfer, M. Sener and K. Schulten, *J. Phys. Chem. Lett.*, 2011, **3**, 526.
- [3] G. D. Scholes and C. Smyth, *J. Chem. Phys.*, 2014, **140**, 110901.
- [4] D. M. Eisele, S. Kirstein, J. Knoester, J. P. Rabe and D. A. Vanden Bout, *Nature Nanotechnology*, 2009, **4**, 658.
- [5] D. M. Eisele, C. W. Cone, E. A. Bloemsma, S. M. Vlaming, C. G. F. van der Kwaak, R. J. Silbey, M. G. Bawendi, J. Knoester, J. P. Rabe and D. A. Vanden Bout, *Nature Chemistry*, 2012, **4**, 655.
- [6] T. Fujita, J. C. Brookes, S. K. Saikin and A. Aspuru-Guzik, *J. Phys. Chem. Lett.*, 2012, **3**, 2357.
- [7] J. M. Linnanto and E. I. Korppi-Tommola, *J. Phys. Chem. B*, 2013, **117**, 11144.
- [8] J. Huh, S. K. Saikin, J. C. Brookes, S. Valleeau, T. Fujita, and A. Aspuru-Guzik, *J. Am. Chem. Soc.*, 2014, **136**, 2048.
- [9] F. Würthner, T. E. Kaiser and C. R. Saha-Möller, *Angewandte Chemie International Edition*, 2011 **50**, 3376.
- [10] H. Lin, R. Camacho, Y. Tian, T. E. Kaiser, F. Würthner and I. G. Scheblykin, *Nano Lett.*, 2010, **10**, 620.
- [11] S. Liu, D. Schmitz, S.-S. Jester, N. J. Borys, S. Höger and J. M. Lupton, *J. Phys. Chem. B*, 2013, **117**, 4197.
- [12] A. V. Aggarwal, A. Thiessen, A. Idelson, D. Kalle, D. Würsch, Th. Stangl, F. Steiner, S.-S. Jester, J. Vogel-sang, S. Höger and J. M. Lupton, *Nature Chemistry*, 2013, **5**, 964.
- [13] E.A. Ermilov, S. Hackbarth, S. Al-Omari, M. Helmreich, N. Jux, A. Hirsch and B. Röder, *Optics Communications*, 2005, **250**, 95.
- [14] J. Megow, T. Renger and V. May, *ChemPhysChem*, 2014, **15**, 478.
- [15] 5,6-Dichloro-2-[3-[5,6-dichloro-1-octyl-3-(2-sulfopropyl)-benzimidazol-2-ylidene]-propenyl]-1-octyl-3-(2-sulfopropyl)-benzimidazolium hydroxide
- [16] H. v. Berlepsch, S. Kirstein, R. Hania, A. Pugžlys and C. Böttcher, *The Journal of Physical Chemistry B*, 2007, **111**, 1701.
- [17] H. v. Berlepsch, K. Ludwig, S. Kirstein, and C. Böttcher, *Chemical Physics*, 2011, **385**, 27.
- [18] K. A. Clark, C. W. Cone and D. A. Vanden Bout, *The Journal of Physical Chemistry C*, 2013, **117**, 26473.
- [19] C. Didraga, A. Pugžlys, P. R. Hania, H. v. Berlepsch, K. Duppen and J. Knoester, *The Journal of Physical Chemistry B*, 2004, **108**, 14976.
- [20] A. Pugžlys, R. Augulis, P. H. M. van Loosdrecht, C. Didraga, V. A. Malyshev and J. Knoester, *The Journal of Physical Chemistry B*, 2006, **110**, 20268.
- [21] S. M. Vlaming, E. A. Bloemsma, M. L. Nietiadi and J. Knoester, *J. Chem. Phys.*, 2011, **134**, 114507.
- [22] D.M. Eisele, D. H. Arias, X. Fu, E. A. Bloemsma, C. P. Steiner, R. A. Jensen, P. Rebentrost, H. Eisele, A. Tokmakoff, S. Lloyd, K. A. Nelson, D. Nicastro, J. Knoester and M. G. Bawendi, *PNAS*, 2014, **111**, E3367.
- [23] F. Haverkort, A. Stradomska, A., A. H. de Vries and J. Knoester, *J. Phys. Chem. A*, 2014, **118**, 1012.
- [24] F. London, *Trans. Farad. Soc.*, 1937, **33**, 8.
- [25] H. Zoubi, A. Eisfeld and S. Wüster, *Phys. Rev. A*, 2014, **89**, 053426.
- [26] The MD simulations have been carried out using NAMD [44] together with the AMBER force field [45] as well as the GAFF parameter sets [46]. The MD-simulations are carried out in a periodic box, the electrostatic interactions were computed using the particle mesh Ewald method [47]. The temperature was heated to 300 K and 7 ns of MD simulation with a time-step of 0.5 fs was carried out.
- [27] J. Megow, T. Körzdörfer, M. Sparenberg, T. Renger, S. Blumstengel, F. Henneberger and V. May, *arXiv:1411.2818* [cond-mat.mtrl-sci].
- [28] W. Humphrey, A. Dalke and K. Schulten, *Journal of Molecular Graphics*, 1996, **14**, 33.
- [29] J. Megow, A. Kulesza, Z. wang Qu, T. Ronneberg, V. Bonačić-Koutecký and V. May, *Chem. Phys.*, 2010, **377**, 10.
- [30] The partial charges have been computed (see [39]). The differential dipole moment  $\Delta d$  was fitted to the result of hole burning experiments for similar cyanine dyes ( $0.7D < |\Delta d| < 1.1D$ ) [48]. We chose  $\Delta d = 1D$  and we note that other values within the range will change the absorption spectrum only slightly.
- [31] V. May and O. Kühn, *Charge and Energy Transfer Dynamics in Molecular Systems*, WILEY-VHC, 2011
- [32] T. Renger and F. Müh, *Phys. Chem. Chem. Phys.*, 2013, **15**, 3348.



- [33] N. S. Bayliss, *J. Chem. Phys.*, 1950, **18**, 292.
- [34] L. Wenyuan, Z. Fushi, T. Yingwu and S. Xinqi, *Act. Phys.-Chim. Sin.*, 1985, **1**, 12.
- [35] V. V. Shelkovnikov and A. I. Plekhanov, Optical and Resonant Non-Linear Optical Properties of J-Aggregates of Pseudoisocyanine Derivatives in Thin Solid Film. In *Macro To Nano Spectroscopy*,; Uddin, D. J., Ed.; In-Tech,; 2012.
- [36] T. Renger, B. Grundkötter, M. E.-A. Madjet and F. Müh, *Proc. Natl. Acad. Sci.*, 2008, **105**, 13235.
- [37] M. E. Madjet, A. Abdurahman and T. Renger, *J. Phys. Chem. B*, 2006, **110**, 17268-17281 PMID: 16928026.
- [38] J. Adolphs, F. Müh, M. E.-A. Madjet and T. Renger, *Photosynth Res*, 2008, **95**, 197-209.
- [39] The geometry of the monomeric cyanine dye has been optimized at the DFT level, the absorption energy for the first excited state has been calculated in the frame of TDDFT employing the long-range corrected hybrid CAM-B3LYP functional [49] and the TZVP atomic orbital basis set [50] for all atoms. Atomically centered partial charges (electronic ground and first excited state) and transition charges (only for heavy atoms) have been fitted to the electrostatic potential of the respective charge/transition charge density by using the CHELPG procedure [51].
- [40] F. Milota, V.J. Prokhorenko, T. Mancal, H. v. Berlepsch, O. Bixner, H.F. Kauffmann and J. Hauer, *J. Phys. Chem. A*, 2013, **117**, 6007-6014.
- [41] F. C. Spano, *J. Chem. Phys.*, 2002, **116**,.
- [42] F. C. Spano, *Accounts of Chemical Research*, 2010, **43**, 429-439 PMID: 20014774.
- [43] A. Merdasa, Á.J. Jiménez, R. Camacho, M. Meyer, F. Würthner and I.G. Scheblykin, *Nano Letters*, 2014,**14**, 6774.
- [44] J. C. Phillips, R. Braun, W. Wang, J. Gumbart, E. Tajkhorshid, E. Villa, C. Chipot, R. D. Skeel, L. Kale and K. Schulten, *J. Comput. Chem.*, 2005, **26**, 1781-1802.
- [45] D. A. Case *et al.*, "AMBER 8", University of California, San Francisco, CA, 2004.
- [46] J. Wang, R. M. Wolf, J. W. Caldwell, P. A. Kollman and D. A. Case, *J. Comput. Chem.*, 2004, **25**, 1157-1174.
- [47] T. Darden, D. York and L. Pedersen, *J. Chem. Phys.*, 1993, **98**, 10089-10092.
- [48] A. Chowdhury, S. Wachsmann-Hogiu, P. R. Bangal, I. Raheem and L. A. Peteanu, *J. Phys. Chem. B*, 2001, **105**, 12196-12201.
- [49] T. Yanai, D. P. Tew and N. C. Handy, *Chem. Phys. Lett.*, 2004, **393**, 51.
- [50] F. Weigend and R. Ahlrichs, *Phys. Chem. Chem. Phys.*, 2005, **7**,, 3297.
- [51] M. Breneman and K. B. Wiberg, *J. Comput. Chem.*, 1990, **11**, 361.